Synthetic Metals 161 (2011) 1–6

Contents lists available at ScienceDirect

Synthetic Metals

journal homepage: www.elsevier.com/locate/synmet

Synthesis of random copolymers based on 3-hexylthiophene and quinoxaline derivative: Influence between the intramolecular charge transfer (ICT) effect and π-conjugation length for their photovoltaic properties

Jang Yong Lee, Min Hee Choi, Soo Won Heo, Doo Kyung Moon *

Department of Materials Chemistry and Engineering, Konkuk University, 1 Hwayang-dong, Gwangjin-gu, Seoul 143-701, Republic of Korea

ARTICLE INFO

Article history:
Received 6 April 2010
Received in revised form 30 July 2010
Accepted 18 August 2010
Available online 27 November 2010

Keywords:
Organic photovoltaics
Charge transfer
Conjugated polymers
Copolymerization

ABSTRACT

A series of low band gap, donor–acceptor polymers composed of regioregular 3-hexylthiophene segments and quinoxaline derivative units were synthesized by Stille coupling polymerization. The polymers had relatively low optical band gaps ranging from 1.61 to 1.83 eV. A bulk-heterojunction structure of glass/indium–tin oxide (ITO)/PEDOT:PSS/polymer-PCBM (1:3)/BaF_2/Ba/Al was fabricated to examine the photovoltaic properties. 1-(3-Methoxycarbonyl)propyl-1-phenyl-[6,6]-C-71 ($PC_{71}BM$) was used as the acceptor material owing to its increased absorption property in the visible region compared to 1-(3-methoxycarbonyl)propyl-1-phenyl-[6,6]-C-61 ($PC_{61}BM$). Among these polymers, P1 showed the best device performance with a PCE of 0.88%. These results provided an effective strategy for the design and synthesis of low band gap conjugated polymers with a broad range of absorption.

1. Introduction

π-Conjugated polymers involving a variety of aromatic rings have potential applications, such as organic light-emitting diodes (OLEDs) [1–5], organic thin-film transistors (OTFTs) [6–9], and organic photovoltaics (OPVs) [10–21]. In particular, OPVs have generated considerable scientific interest due to a potential in fabricating low-cost integrated circuit elements for large area and the feasibility of low production using various methods such as spin-coating, ink-jet printing, and roll-to-roll through solution process [22–28]. Since donor polymers have been investigated for OPVs, poly(3-hexylthiophene) (P3HT) has been considered to be a most efficient polymer material. Considerable efforts to optimize the processing conditions, such as the acceptor molar ratio and different annealing conditions, have resulted in power conversion efficiencies of approximately 5% [29,30]. Recently, various polymer materials have been studied extensively to enhance the photovoltaic efficiency and oxidative stability by reducing the band gap and optimizing the highest occupied molecular orbital (HOMO) and the lowest unoccupied molecular orbital (LUMO) energy levels [31–34]. Nevertheless, P3HT is still regarded as one of the most important organic semiconductor materials owing to its good planarity, hole mobility, solubility and power conversion efficiency (PCE). However, P3HT has a restricted absorption range of the solar spectrum on account of its relatively large band gap (~2 eV) [35]. In addition to the absorption spectrum of P3HT, its high crystallinity makes it form large crystalline domains, which reduce the interfacial area available for charge separation, resulting in low efficiency devices. Moreover, it may be a limiting factor for the large area fabrication of solar cells. If an efficient n-type monomer can be introduced in the P3HT backbone, the polymer band gap could be reduced via an intramolecular charge transfer (ICT) effect [36–39]. Furthermore, the regio-irregularity of the polymer resulting from the n-type monomer in the P3HT backbone effectively controls the crystallinity of polymer, which can enhance the interfacial properties between the donor and acceptor materials.

In this study, low band gap polymers were developed by introducing a frequently used electron-deficient unit into the poly(3-hexylthiophene) main chain to reduce the band gap, which improved the interchain packing, solubility and optimized the ICT effects. Quinoxaline derivative, which is an excellent electron attraction unit, was introduced as a n-type monomer. Furthermore, a hexyloxyphenyl side chain was adopted in the quinoxaline unit to increase the solubility and resonance properties. In polymerization, the molar ratio of 3-hexylthiophene was controlled to optimize the effective π-conjugation length of the 3-hexylthiophene oligomer. A thiophene spacer was introduced into the polymer skeleton to control the orientation of the alkyl chains and reduce steric hindrance between the 3-hexylthiophene oligomer moiety and electron withdrawing moiety. 2,5-Bis(trimethyl stannyl)thiophene and 2,3-Bis(4-hexyloxyphenyl)-5,8-dibromoquinoxaline were dissolved in a solvent and stirred for 1 h under mild heating conditions

* Corresponding author. Tel.: +82 2 450 3498; fax: +82 2 444 0765.
E-mail address: dkmoon@konkuk.ac.kr (D.K. Moon).

0379-6779/$ – see front matter © 2010 Elsevier B.V. All rights reserved.
doi:10.1016/j.synthmet.2010.08.012

so that the thiophene spacer neighbored the quinoxaline delivertive before 2-bromo-3-hexyl-5-trimethylstannylthiophene was added to the mixture. Bulk-heterojunction-type devices were fabricated to examine the photovoltaic properties. $PC_{71}BM$ was introduced as an acceptor material because of its increased absorption in the visible region, which leads to better overlap with the solar spectrum relative to that obtained with the $PC_{61}BM$ [40].

2. Experimental

2.1. Instruments and characterization

Unless specified otherwise, all reagents and chemicals were purchased from Aldrich and used as received. The ^{1}H NMR (400 MHz) spectra were recorded using a Brüker AMX400 spectrometer in $CDCl_3$, and the chemical shifts were recorded in units of ppm with TMS as the internal standard. The elemental analyses were performed with EA1112 using a CE Instrument. The absorption spectra were recorded using an Agilent 8453 UV–visible spectroscopy system. The PL spectra were measured using a Hitachi F-4500 spectrophotometer. The samples used for the UV–visible spectroscopy and photoluminescence (PL) efficiency measurements were dissolved in chloroform at a concentration of 1 mg/ml. The films were drop-coated from the chloroform solution onto a quartz substrate. All GPC analyses were carried out using THF as the eluent and a polystyrene standard as the reference. The TGA measurements were performed using a TA Instrument 2050. The cyclic voltammetry waves were produced using a Zahner IM6eX electrochemical workstation with a 0.1 M acetonitrile (substituted with nitrogen in 20 min) solution containing Bu_4NPF_6 as the electrolyte at a constant scan rate of 50 mV/s. ITO, a Pt wire and silver/silver chloride [Ag in 0.1 M KCl] were used as the working, counter and reference electrodes, respectively. The electrochemical potential was calibrated against Fc/Fc^+. The current–voltage (I–V) curves of the photovoltaic devices were measured using a computer-controlled Keithley 2400 source measurement unit (SMU) equipped with a Peccell solar simulator under an illumination of AM 1.5G (100 mW cm^{-2}).

2.2. Fabrication and characterization of the polymer solar cells

All bulk-heterojunction PV cells were prepared using the following device fabrication procedure. Glass/ITO substrates [Sanyo, Japan(10 Ω/γ)] were sequentially lithographically patterned, cleaned with detergent, and ultrasonicated in deionized water, acetone and isopropyl alcohol. The substrates were dried on a hotplate at 120 °C for 10 min and treated with oxygen plasma for 10 min to improve the contact angle immediately before the film coating process. Poly(3,4-ethylene-dioxythiophene):poly(styrenesulfonate) (PEDOT:PSS, Baytron P 4083 Bayer AG) was passed through a 0.45 μm filter before being deposited onto ITO at a thickness of ca. 32 nm by spin-coating at 4000 rpm in air and then dried at 120 °C for 20 min inside a glove box. A mixture of the polymers/PCBM 1:3 (w/w), 5.0 mg ml^{-1} in chlorobenzene was stirred overnight, filtered through a 0.45 μm poly(tetrafluoroethylene) (PTFE) filter, and then spin-coated (1100 rpm, 40 s) on top of the PEDOT:PSS layer. The sample was then heated to 120 °C for 10 min inside a glove box filled with nitrogen. Device fabrication was completed by depositing thin layers of BaF_2 (1 nm), Ba (2 nm) and Al (200 nm) at <10^{-6} Torr. The active area of the device was 9 mm^2. Finally, the cell was encapsulated with UV-curing glue (Nagase, Japan). The illumination intensity was calibrated using a standard Si photodiode detector equipped with a KG-5filter. The output photocurrent was adjusted to match the photocurrent of the Si reference cell to obtain a power density of 100 mW cm^{-2}. After encapsulation, all devices were operated under an ambient atmosphere at 25 °C.

2.3. Synthesis of monomers

2.3.1. 2,3-Bis(4-hexyloxyphenyl)-5,8-dibromoquinoxaline. 5

Aqueous potassium hydroxide (4 equiv.) was added to a solution of 4 (3.58 g, 7.6 mmol) in ethanol (50 ml). The mixture was stirred for 1 h at room temperature and n-bromohexane was added. The reaction mixture was allowed to react at 70 °C for 24 h, and cooled to −20 °C. After filtration, the crude product was purified by recrystallization from methanol to give a yellow solid (2.35 g, 48%). ^{1}H NMR ($CDCl_3$, 400 MHz) δ 7.85 (s, 2H), 7.65 (d, J = 8 Hz, 4H), 6.88 (d, J = 8 Hz, 4H), 3.99 (t, J = 6 Hz, 4H), 1.79 (m, J = 6 Hz, 4H), 1.48 (m, J = 6 Hz, 4H), 1.34 (m, J = 4 Hz, 8H), 0.91 (t, J = 8 Hz, 6H). ^{13}C NMR ($CDCl_3$, 400 MHz) δ 14.5, 23.1, 29.6, 29.7, 30.1, 32.3, 68.8, 114.6, 130.2, 132.9, 133.2, 142.2, 149.8, 157.3, 160.4. Anal. calcd. for $C_{32}H_{36}N_2O_2Br_2$: C, 59.97; H, 5.63; N, 4.38. Found: C, 59.88; H, 5.64; N, 4.33.

2.3.2. 2,5-Bis(trimethyl stannyl)thiophene. 6

2,5-Dibromothiophene (2.75 g, 11.36 mmol) was dissolved in THF (45.4 ml), and the solution was cooled to −50 °C. The 2.5 M solution of n-BuLi in hexane (10 ml, 25 mmol) was added dropwise for 1 h, and the resulting mixture was stirred for 30 min at −50 °C. After 30 min, the solution was cooled to −78 °C, and a 1.0 M solution of Me_3SnCl in THF (25 ml, 25 mmol) was added for 1 h. After stirring at −78 °C for 3 h, the solution was allowed to warm to room temperature and stirred for 24 h. This mixture was then poured into n-hexane, washed with $NaHCO_3$ and water twice and dried over Na_2SO_4. The solvents were removed by rotary evaporation to afford a brown solid. The crude product was recrystallized with hexane to produce light-brown crystals (2.79 g, 60%). ^{1}H NMR ($CDCl_3$, 400 MHz) δ 7.37 (s, 2H), 0.36 (t, J = 27.4 Hz, 18H).

2.3.3. 2-Bromo-3-hexyl-5-trimethylstannylthiophene. 7

2-Bromo-3-hexylthiophene (12 g, 50 mmol) was dissolved in THF (41 ml) and cooled to −78 °C. A 2.0 M solution of lithium diisopropylamine in THF (28 ml, 56 mmol) was added dropwise over a 1 h period. After stirring for 1 h at −78 °C, a 1.0 M solution of Me_3SnCl in THF (56 ml, 56 mmol) was added dropwise, and the mixture was stirred at −50 °C for 2 h. The solution was allowed to warm to room temperature and stirred for 24 h. After the reaction was complete, the reaction mixture was poured into water and extracted with ether. The organic phase was washed several times with brine and dried over Na_2SO_4. The solvents were removed by rotary evaporation to afford a brown liquid. The residue was reduced-distilled to produce the product as a colorless oil in 76% yield (15.6 g). ^{1}H NMR ($CDCl_3$, 400 MHz): δ 6.85 (s, 1H), 2.55 (t, J = 7.6 Hz, 2H), 1.56 (t, J = 7.2 Hz, 2H), 1.31 (m, 6H), 0.88 (t, J = 6.8 Hz, 3H), 0.36 (t, J = 27.6 Hz, 9H). ^{13}C NMR (DMSO-d_6, 400 MHz): −7.56 (m), 14.75, 23.28, 29.73, 29.95, 30.54, 32.31, 114.12, 136.97(m), 138.62, 143.80.

2.4. General procedure of polymerization through the stille reaction

Equimolar amounts (0.47 mmol) of 2,5-Bis(trimethyl stannyl)thiophene and 2,3-Bis(4-hexyloxyphenyl)-5,8-dibromoquinoxaline were dissolved in DMF (0.125 M). After mild heating for 1 h, different amounts of 2-bromo-3-hexyl-5-trimethylstannylthiophene (P1: 1.41 mmol, P2: 2.82 mmol, P3: 5.64 mmol, P4: 8.46 mmol) were added. Subsequently, 1.25 mol% of $Pd(PPh_3)_2Cl_2$ was added to the mixture. The orange solution was warmed to 120 °C and allowed to reflux for 48 h under N_2. 2-Bromo thiophene was added systematically to the end-cap of the polymer chain. After cooling to room temperature, the polymer was poured into methanol (300 ml) and filtered. The filtered polymer was further dissolved in $CHCl_3$, reprecipitated into methanol and filtered again. The polymer was further purified by washing with

methanol, acetone and hexane in a Soxhlet apparatus for 24 h. The chloroform soluble fraction was recovered and dried under a reduced pressure at 50 °C.

2.4.1. P1

Black solid 0.47 g (yield = 44%). ^{1}H NMR ($CDCl_3$, 400 MHz) δ 8.04 (quinoxailne-H), 7.65–7.89 (thiophene, phenyl-H), 6.91 (phenyl-H), 4.00 (–OCH_2), 2.6–2.8 (thiphene-CH_2), 1.81 (CH_2), 1.32–1.54 (CH_2), 0.93 (CH_3). Anal. calcd. for $C_{66}H_{80}N_2S_4O_2$: C, 74.44; H, 7.52; N, 2.63; S, 12.03; O, 3.38. Found: C, 73.52; H, 7.48; N, 2.64; S, 12.08; O, 3.52.

2.4.2. P2

Black solid 0.65 g (yield = 40%). ^{1}H NMR ($CDCl_3$, 400 MHz) δ 8.04 (quinoxailne-H), 7.65–7.89 (thiophene, phenyl-H), 6.91 (phenyl-H), 4.00 (–OCH_2), 2.6–2.8 (thiphene-CH_2), 1.81 (CH_2), 1.32–1.54 (CH_2), 0.93 (CH_3). Anal. calcd. for $C_{96}H_{122}N_2S_7O_2$: C, 73.94; H, 7.83; N, 1.80; S, 14.38; O, 2.05. Found: C, 73.48; H, 7.62; N, 1.78; S, 14.44; O, 2.16.

2.4.3. P3

Black solid 1.26 g (yield = 49%). ^{1}H NMR ($CDCl_3$, 400 MHz) δ 8.04 (quinoxailne-H), 7.65–7.89 (thiophene, phenyl-H), 6.91 (phenyl-H), 4.00 (–OCH_2), 2.6–2.8 (thiphene-CH_2), 1.81 (CH_2), 1.32–1.54 (CH_2), 0.93 (CH_3). Anal. calcd. for $C_{155}H_{206}N_2S_{13}O_2$: C, 73.3; H, 8.07; N, 1.09; S, 16.29; O, 1.25. Found: C, 73.07; H, 8.02; N, 1.08; S, 16.18; O, 1.31.

2.4.4. P4

Black solid 1.65 g (yield = 38%). ^{1}H NMR ($CDCl_3$, 400 MHz) δ 8.04 (quinoxailne-H), 7.65–7.89 (thiophene, phenyl-H), 6.91 (phenyl-H), 4.00 (–OCH_2), 2.6–2.8 (thiphene-CH_2), 1.81 (CH_2), 1.32–1.54 (CH_2), 0.93 (CH_3). Anal. calcd. for $C_{216}H_{290}N_2O_2S_{19}$: C, 73.01; H, 8.17; N, 0.79; S, 17.13; O, 0.9. Found: C, 72.88; H, 8.09; N, 0.77; S, 17.06; O, 1.09.

3. Results and discussion

3.1. Synthesis and characterization

Chloroform was dried over $CaCl_2$, and diethyl ether, THF and toluene were dried over sodium under a nitrogen atmosphere. The other reagents and chemicals were used as received. 4,7-Dibromo-2,1,3-benzothiadiazole [41], 3,6-dibromo-1,2-phenylenediamine [42], 2,3-Bis(4-methoxyphenyl)-5,8-dibromoquinoxaline [15], 2,3-Bis(4-hydroxyphenyl)-5,8-dibromoquinoxaline [15] were prepared as described in the literature.

Scheme 1 shows the synthesis process for the monomers and polymers. 3-Hexylthiophene was brominated with N-bromosucsinimide (NBS) and then stannated with trimethyltinchloride to produce 4. P1–P4 were synthesized through a Stille coupling reaction using $Pd(PPh_3)_2Cl_2$ as the catalyst in N,N′-dimethyl formamide (DMF). Each polymer was well dissolved in common organic solvents, such as chloroform, THF, toluene, chlorobenzene (CB) and dichlorobenzene (DCB).

The molecular weight of the polymers was measured by GPC, and polystyrene was used as the standard with THF as the eluent. The number of average molecular weight (Mn) increased with increasing 3-hexylthiophene ratio in the polymer backbone because of the increased solubility of the polymers caused by the larger number of alkyl side chains in the polymer skeletons. The thermal properties of these copolymers were examined by thermogravimetric analysis (TGA) at a heating rate of 10 K/min. As shown in Fig. 1, P2 had a decomposition temperature (T_d) near 380 °C, whereas T_d of the others (P1, P3, P4) was approximately 410 °C. This suggests that these polymers exhibited good thermal stability, making them suitable for use in polymer solar cells and other optoelectronic devices. Table 1 lists the results of the molecular weight measurements and thermal properties.

3.2. Optical and electrochemical properties

Fig. 2 shows the UV–vis absorption spectrum of P1–P4 in the chloroform solution and thin solid films. P1 and P2 in solution exhibited maximum UV–vis absorption peaks (λ_{max}) at 329/566 nm and 404/508 nm, respectively. The λ_{max} of P3 and P4 were observed at 433 and 439 nm, respectively. In the films, UV–vis absorption λ_{max} of P1–P4 were observed at 322/603, 412/538, 508 and 500 nm, respectively. All the polymers showed red-shift in absorption, which indicates that these polymers have good intermolecular stacking properties in film form. The polymers that had a small molar ratios of 3-hexylthiophene in the polymer backbone, such as P1 and P2, showed UV–vis absorption spectra in the longer

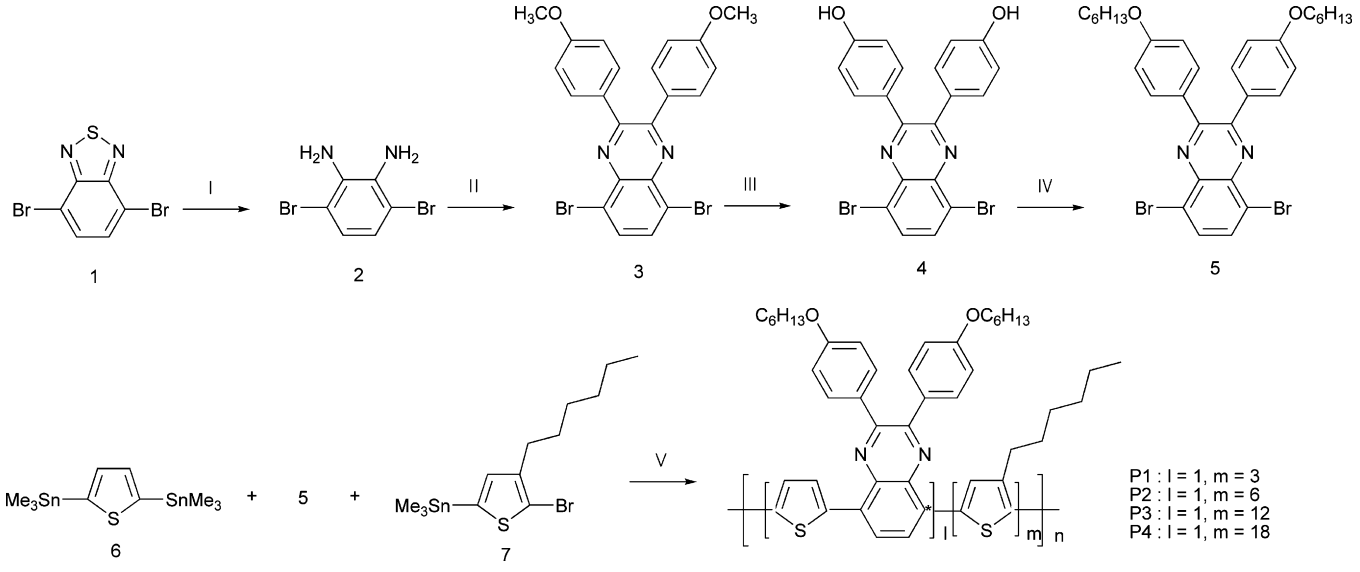

Scheme 1. The synthetic routes of the monomers and polymers. (I) $NaBH_4$, ethanol; (II) 4,4′-dimethoxybenzil, butanol; (III) C_5H_5N·HCl, reflux; (IV) n-bromohexane, ethanol, reflux; (V) DMF, $Cl_2(PPh_3)_2Pd$, reflux.

Table 1
Molecular weights and thermal properties of the synthesized polymers.

Polymer	Q[a]:3HT[b] molar ratio	Yield (%)	M_n	M_w	M_w/M_n	T_d (°C)
P1	1:3	44	24,593	35,009	1.42	409
P2	1:6	40	43,926	54,678	1.24	382
P3	1:12	49	52,570	60,948	1.16	409
P4	1:18	38	88,384	122,572	1.38	409

Molecular weights and polydispersity indexes determined by GPC in THF on the basis of polystyrene calibration.
[a] Quinoxaline derivative.
[b] 3-Hexylthiophene.

wavelength range. This was attributed to the ICT effect. The high molar ratio of electron withdrawing moieties results in an efficient ICT effect between the quinoxaline moiety and 3-hexylthiophene. However, the polymers showed an increasing red-shift in absorption with increasing molar ratio of 3-hexylthiophene. Moreover, the UV–vis absorption spectra of the polymers with high molar ratios of 3-hexylthiophene in the polymer backbone, such as P3 and P4, showed similar behavior to P3HT with increasing 3-hexylthiophene molar ratio. This originates from the improved crystallinity. Considering that most of the photons in the solar spectrum range from 500 to 900 nm, the photocurrent density and incident photon-to-current conversion efficiency (IPCE) of P1 are expected to be better than the other polymers. The optical band gap was calculated from the band edge of the UV–vis absorption spectrum in the film. The polymers had a relatively low optical band gap of 1.61–1.83 eV. Among these polymers, P1, which had the lowest 3-hexylthiophene molar ratio of the four polymers, exhibited the lowest band gap. P1 could effectively develop orbital overlap due to the ICT effect.

Fig. 3 presents the PL spectra of the polymers. In solution, the four polymers had maximum emission peaks ranging from 660 to 680 nm. Solid-state photoluminescence was observed in the red emission region with the maximum emission peaks in the range from 710 to 730 nm. Four polymers showed red-shifted maximum emission peaks of approximately 50 nm. It appears that the four polymers have strong intermolecular interactions in film form, which allow these polymers to have good stacking properties.

The electrochemical behavior of the copolymers was examined by cyclic voltammetry (CV). The HOMO levels of the polymers were determined using the oxidation onset value. The levels were estimated here on the basis of the reference energy level of ferrocene (4.8 eV below the vacuum level), according to the following equation:

$$E^{HOMO} = [-(E_{onset} \text{ vs. Ag/AgCl}) - E_{onset}(Fc/Fc^{+} \text{ vs. Ag/AgCl})] - 4.8\,eV$$

The LUMO levels were calculated from the offset between the HOMO energy levels and optical band gaps, which was determined using the UV–vis absorption onset value in the films. Fig. 4 shows cyclic voltammograms of the synthesized polymers. According to these results, the HOMO of the synthesized

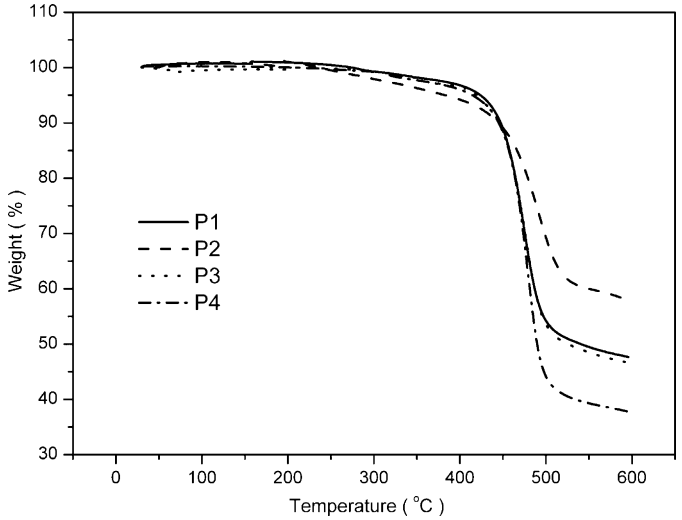

Fig. 1. TGA curves of the polymers.

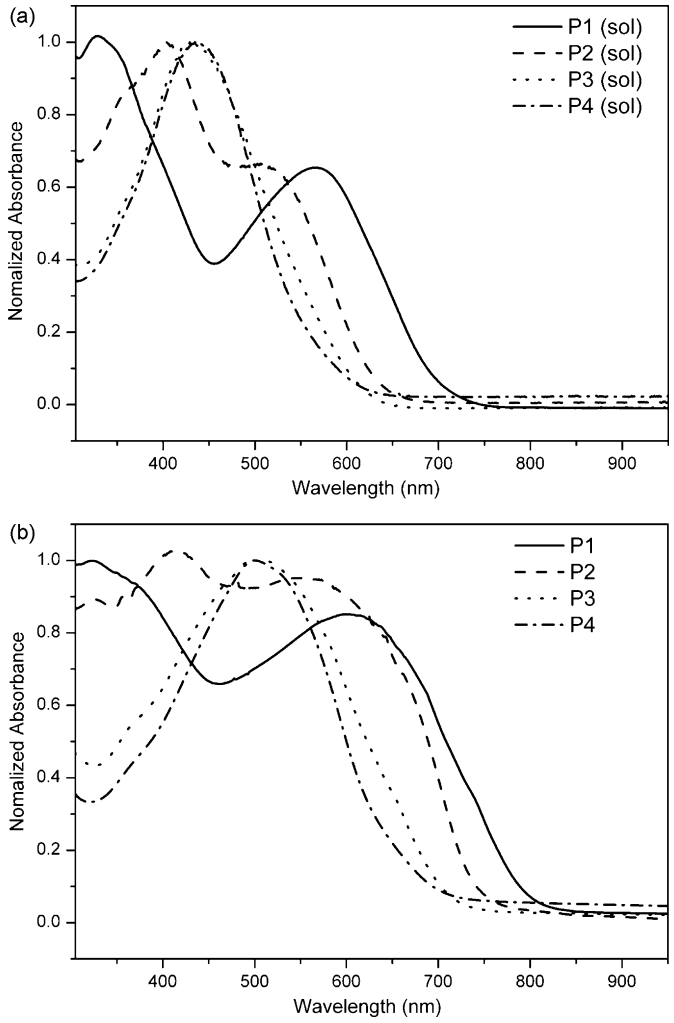

Fig. 2. UV–vis absorption spectra of the polymers (a) in solution and (b) in film.

Table 2
Optical, electrochemical data and energy levels of the four polymers.

Polymer	Absorption λ_{max} (nm)[a]		PL λ_{max} (nm)[d]		E_g^{op}[e] (eV)	E_{onset}^{ox}[f]	Energy level (eV)[g]	
	Solution[b]	Film[c]	Solution[b]	Film[c]			HOMO	LUMO
P1	329, 566	322, 603	661	711	1.61	0.53	−4.98	−3.37
P2	404, 508	412, 538	680	721	1.67	0.57	−5.02	−3.35
P3	433	508	670	720	1.73	0.58	−5.03	−3.3
P4	439	500	677	730	1.83	0.58	−5.03	−3.2

[a] λ_{max} was determined from UV–vis data.
[b] Diluted in chloroform.
[c] Spin-coated from a chloroform.
[d] λ_{max} was determined from PL data.
[e] Estimated from the onset of UV–vis absorption data of the thin-film.
[f] Onset oxidation potential.
[g] Calculated from the reduction and oxidation potentials under the assumption that the absolute energy level of Fc/Fc^+ was 4.8 eV below a vacuum.

polymers was −4.98 to −5.03 eV, and the LUMO was −3.2 to −3.37 eV. The LUMO and band gap increased with increasing 3-hexylthiophene molar ratio in the polymer backbone due to the reduced ICT effect. In other words, the molecular orbital overlapping effect between the electron withdrawing moiety and electron donating moiety became stronger with decreasing 3-hexylthiophene molar ratio, which gave the polymer a lower LUMO and band gap. Based on these optical and electrochemical measurements, P1 would be the best active material for OPVs. Table 2 summarizes the optical and electrochemical properties of the polymers.

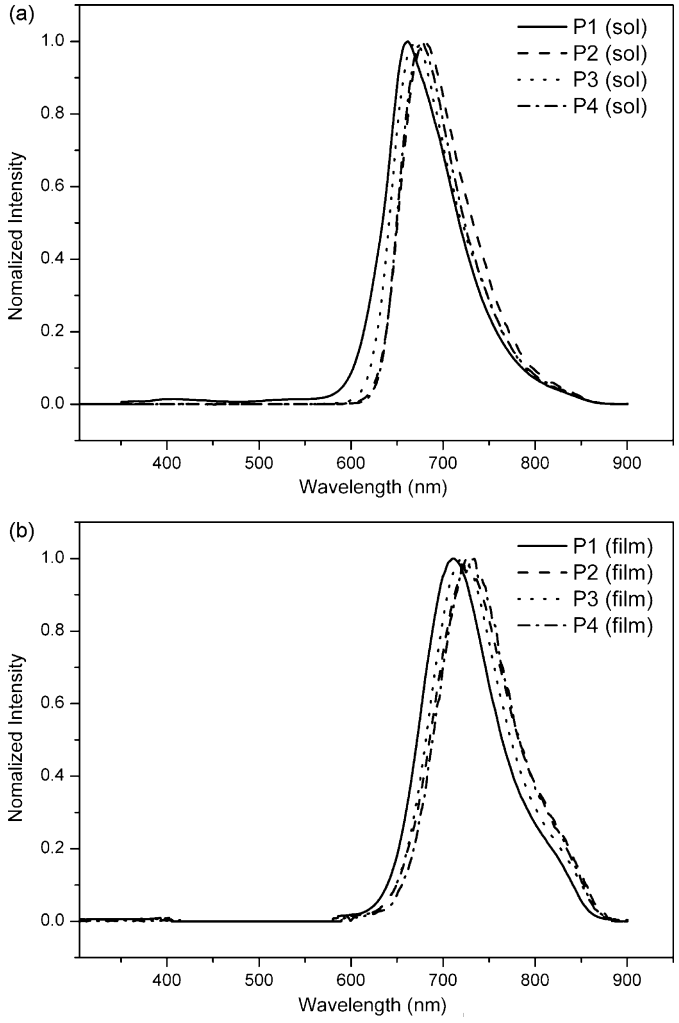

Fig. 3. Comparison of the PL spectra of the polymers (a) in solution and (b) in film.

3.3. Photovoltaic properties

All synthesized polymers were applied to the bulk-heterojunction geometry (BHG) with PCBM. The OPV cells were fabricated with a sandwiched glass/ITO/PEDOT:PSS/polymer–PCBM (1:3, w:w)/BaF_2/Ba/Al structure. A blend of the polymer (5.0 mg ml^{-1} of the polymer in chlorobenzene (CB)) and $PC_{71}BM$ was dissolved in CB, filtered through a 0.45 μm poly(tetrafluoroethylene) (PTFE) filter, and spin-coated at 1100 rpm for 40 s. The active layers were preannealed at 120 °C for 10 min before electrode deposition. Each substrate was patterned using photolithography techniques to produce a segment with an active area of 9.0 mm^2. After encapsulating the fabricated devices in a glove box, the *I–V* characteristics were measured under an ambient atmosphere.

Fig. 5 shows the *I–V* properties of the fabricated devices. $PC_{71}BM$ were introduced as acceptor materials because it has increased solubility and absorption properties in the visible region over $PC_{61}BM$. P1–P4 exhibited V_{OC} values of 0.535–0.677 V and J_{SC} values of 1.32–4.35 mA/cm^2. As expected, the best performance was observed in the device that used the P1/$PC_{71}BM$ blend film as the active layer, corresponding to a V_{OC}, J_{SC}, FF and PCE of 0.535 V, 4.35 mA/cm^2, 0.38% and 0.88%, respectively. The PCE values of the four polymers decreased with increasing molar ratio of 3-hexylthiophene in a polymer skeleton. This stems from a decrease in the ICT effect. A decrease in the ICT effect results in inferior photon absorption properties in the long wavelength range and increases the LUMO energy levels. The restricted absorption range of the solar spectrum and high LUMO energy level can decrease

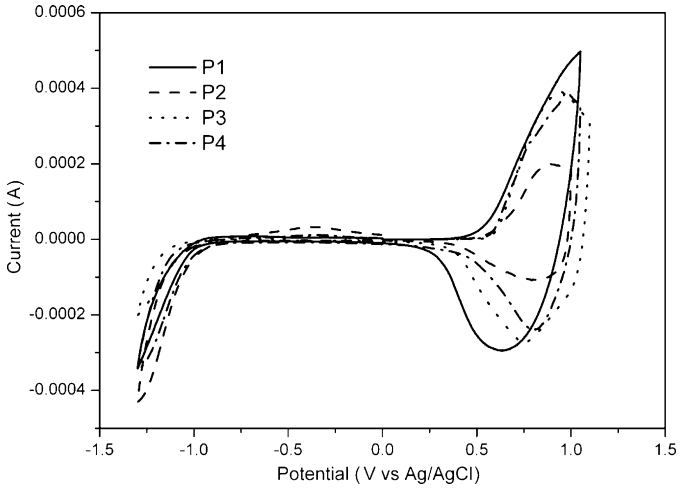

Fig. 4. Cyclic voltammograms of thin films recorded in 0.1 M Bu_4NPF_6/acetonitrile at a scan rate of 50 mV/s.

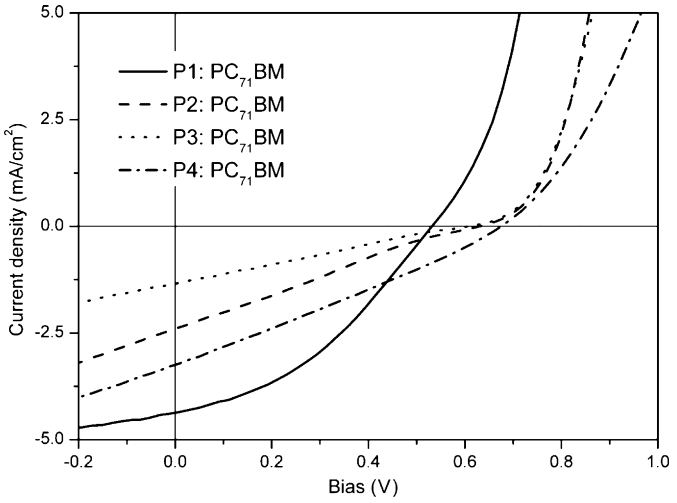

Fig. 5. *I–V* characteristics of photovoltaic devices (polymer:$PC_{71}BM$ = 1:3) with polymer/$PC_{71}BM$ blend films as active layers.

Table 3
Photovoltaic characteristics of the devices that have polymer/$PC_{71}BM$ blend films as the active layers.

Polymer	Jsc (mA/cm^2)[a]	V_{oc} (V)[a]	FF[a]	η (%)[a]
P1[b]	4.35	0.535	0.38	0.88
P2[b]	2.36	0.636	0.24	0.35
P3[b]	1.32	0.616	0.25	0.21
P4[b]	3.21	0.677	0.28	0.60

[a] Under AM 1.5 simulated solar illumination at an irradiation intensity of 100 mW/cm^2.
[b] Using a $PC_{71}BM$ as a acceptor (polymer:$PC_{71}BM$ = 1:3, w/w).

the current density. However, the PCE value of P4 was higher than that of P3. Although the ICT effect decreased with increasing 3-hexylthiophene molar ratio in the polymer skeleton, the improved structural regularity and conjugation length of P4 led to higher current density values than that of P3. In other words, the low PCE value of P3 is due to the reduced ICT effect and the structural irregularity. In particular, the better performance of these devices may be due to an improvement in structural regularity, which resulted in improved intermolecular interactions. Overall, the current density of the five polymers influenced the optical properties and nature of the intermolecular structure. Table 3 lists the photovoltaic properties of the polymers.

4. Conclusions

D-A type copolymers, based on 3-hexylthiophene and 2,3-Bis(4-hexyloxyphenyl)-5,8-dibromoquinoxaline, were synthesized using the Stille coupling reaction for OPVs. These copolymers exhibited low band gaps of 1.61–1.83 eV and PCE values of 0.21–0.88%. Among these polymers, P1 had a low band gap (1.61 eV) and PCE value of 0.88% (V_{OC} = 0.537 V, J_{SC} = 4.35 mA/cm^2, FF = 0.38). The PCE values of the four polymers decreased with increasing 3-hexylthiophene molar ratio in the polymer skeleton. This was attributed to a decrease in the ICT effect. The PCE value of P4 was higher than that of P3 due to a increase in the conjugation length and crystallinity.

Acknowledgement

This work was supported by the New and Renewable Energy R&D program (2008-N-PV08-02) under the Korea Ministry of Knowledge Economy (MKE).

References

[1] J. Liu, X. Guo, L. Bu, Z. Xie, Y. Cheng, Y. Geng, L. Wang, X. Jing, F. Wang, Adv. Funct. Mater. 17 (2007) 1917–1925.
[2] J.Y. Lee, Y.J. Kwon, J.W. Woo, D.K. Moon, J. Ind. Eng. Chem. 14 (2008) 810–817.
[3] M.J. Park, J.I. Lee, H.Y. Chu, S.H. Kim, T. Zyung, J.H. Eom, H.K. Shim, D.H. Hwang, Synth. Met. 159 (2009) 1393–1397.
[4] K.W. Song, J.Y. Lee, S.W. Heo, D.K. Moon, J. Nanosci. Nanotechnol. 10 (2010) 99–105.
[5] K.S. Yook, J.Y. Lee, J. Ind. Eng. Chem. 16 (2010) 181–184.
[6] M. Zhang, H.N. Tsao, W. Pisula, C.Y.A.K. Mishra, K. Müllen, J. Am. Chem. Soc. 129 (2007) 3472–3473.
[7] S. Allard, M. Forster, B. Souharce, H. Thiem, U. Scherf, Angew. Chem. Int. Ed. 47 (2008) 4070–4098.
[8] B.S. Ong, Y. Wu, Y. Li, P. Liu, H. Pan, Chem. Eur. J. 14 (2008) 4766–4778.
[9] B.L. Lee, K.M. Han, E.K. Lee, I.N. Kang, D.H. Kim, S. Lee, Synth. Met. 159 (2009) 132–136.
[10] E. Perzon, X. Wang, F. Zhang, W. Mammo, J.L. Delgado, P. de la Cruz, O. Inganäs, F. Langa, M.R. Andersson, Synth. Met. 154 (2005) 53–56.
[11] C. Shi, Y. Yao, Y. Yang, Q. Pei, J. Am. Chem. Soc. 128 (2006) 8980–8986.
[12] M. Jørgensen, K. Norrman, F.C. Krebs, Sol. Energy Mater. Sol. Cells 92 (2008) 686–714.
[13] Y. Li, Y. Zou, Adv. Mater. 20 (2008) 2952–2958.
[14] L. Huo, Z. Tan, X. Wang, Y. Zhou, M. Han, Y. Li, J. Polym. Sci. A: Polym. Chem. 46 (2008) 4038–4049.
[15] J.Y. Lee, W.S. Shin, J.R. Haw, D.K. Moon, J. Mater. Chem. 19 (2009) 4938–4945.
[16] J.Y. Lee, S.W. Heo, H. Choi, Y.J. Kwon, J.R. Haw, D.K. Moon, Sol. Energy Mater. Sol. Cells 93 (2009) 1932–1938.
[17] Y.J. Cheng, S.H. Yang, C.S. Hsu, Chem. Rev. 109 (2009) 5868–5923.
[18] G. Dennler, M.C. Scharber, C.J. Brabec, Adv. Mater. 21 (2009) 1323–1338.
[19] M. Skompska, Synth. Met. 160 (2010) 1–15.
[20] M. Helgesen, R. Søndergaard, F.C. Krebs, J. Mater. Chem. 20 (2010) 36–60.
[21] J.S. Mugridge, R.G. Bergman, K.N. Raymond, J. Am. Chem. Soc. 132 (2010) 1182–1183.
[22] T. Ameri, G. Dennler, C. Lungenschmied, C.J. Brabec, Energy Environ. Sci. 2 (2009) 347–363.
[23] F.C. Krebs, Sol. Energy Mater. Sol. Cells 93 (2009) 394–412.
[24] I. Gonzalez-Valls, M. Lira-Cantu, Energy Environ. Sci. 2 (2009) 19–34.
[25] F.C. Krebs, M. Jørgensen, K. Norrman, O. Hagemann, J. Alstrup, T.D. Nielsen, J. Fyenbo, K. Larsen, J. Kristensen, Sol. Energy Mater. Sol. Cells 93 (2009) 422–441.
[26] F.C. Krebs, S.A. Gevorgyan, J. Alstrup, J. Mater. Chem. 19 (2009) 5442–5451.
[27] F.C. Krebs, S.A. Gevorgyan, B. Gholamkhass, S. Holdcroft, C. Schlenker, M.E. Thompson, B.C. Thompson, D. Olson, D.S. Ginley, S.E. Shaheen, H.N. Alshareef, J.W. Murphy, W.J. Youngblood, N.C. Heston, J.R. Reynolds, S. Jia, D. Laird, S.M. Tuladhar, J.G.A. Dane, P. Atienzar, J. Nelson, J.M. Kroon, M.M. Wienk, R.A.J. Janssen, K. Tvingstedt, F. Zhang, M. Andersson, O. Inganäs, M. Lira-Cantu, R. de Bettignies, S. Guillerez, T. Aernouts, D. Cheyns, L. Lutsen, B. Zimmermann, U. Würfel, M. Niggemann, H. Schleiermacher, P. Liska, M. Grätzel, P. Lianos, E.A. Katz, W. Lohwasser, B. Jannon, Sol. Energy Mater. Sol. Cells 93 (2009) 1968–1977.
[28] F.C. Krebs, T.D. Nielsen, J. Fyenbo, M. Wadstrøm, M.S. Pedersen, Energy Environ. Sci. 3 (2010) 512–525.
[29] M. Reyes-Reyes, K. Kim, D.L. Carroll, Appl. Phys. Lett. 87 (2005) 083506.
[30] M. Reyes-Reyes, K. Kim, J. Dewald, R. López-Sandoval, A. Avadhanula, S. Curran, D.L. Carroll, Org. Lett. 7 (2005) 5749–5752.
[31] D. Mühlbacher, M. Scharber, M. Morana, Z. Zhu, D. Waller, R. Gaudiana, C. Brabec, Adv. Mater. 18 (2006) 2884–2889.
[32] N. Blouin, A. Michaud, D. Gendron, S. Wakim, E. Blair, R. Neagu-Plesu, M. Belletête, G. Durocher, Y. Tao, M. Leclerc, J. Am. Chem. Soc. 130 (2008) 732–742.
[33] J. Hou, H.Y. Chen, S. Zhang, G. Li, Y. Yang, J. Am. Chem. Soc. 130 (2008) 16144–16145.
[34] H.Y. Chen, J. Hou, S. Zhang, Y. Liang, G. Yang, Y. Yang, L. Yu, Y. Wu, G. Li, Nat. Photon 3 (2009) 649–653.
[35] E. Bundgaard, F.C. Krebs, Sol. Energy Mater. Sol. Cells 91 (2007) 954–985.
[36] C. Kitamura, S. Tanaka, Y. Yamashita, Chem. Mater. 8 (1996) 570–578.
[37] G. Brocks, A. Tol, J. Phys. Chem. 100 (1996) 1838–1846.
[38] T. Yamamoto, Z.H. Zhou, T. Kanbara, M. Shimura, K. Kizu, T. Maruyama, Y. Nakamura, T. Fukuda, B.L. Lee, N. Ooba, S. Tomaru, T. Kurihara, T. Kaino, K. Kubota, S. Sasaki, J. Am. Chem. Soc. 118 (1996) 10389–10399.
[39] H.A.M. van Mullekom, J.A.J.M. Vekemans, E.W. Meijer, Chem. Commun. 18 (1996) 2163–2164.
[40] J. Peet, J.Y. Kim, N.E. Coates, W.L. Ma, D. Moses, A.J. Heeger, G.C. Bazan, Nat. Mater. 6 (2007) 497–500.
[41] X. Li, W. Zeng, Y. Zhang, Q. Hou, W. Yang, Y. Cao, Eur. Polym. J. 41 (2005) 2923–2933.
[42] R. Yang, R. Tian, J. Yan, Y. Zhang, J. Yang, Q. Hou, W. Yang, C. Zhang, Y. Cao, Macromolecules 38 (2005) 244–253.